

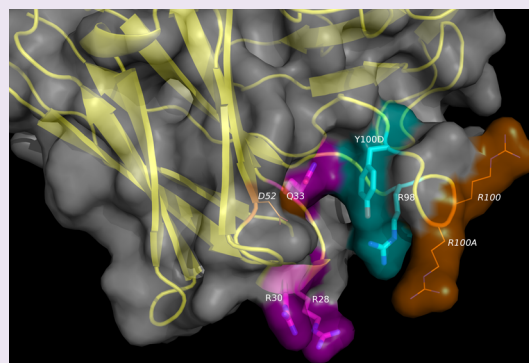
Engineering the Binding Site of an Antibody against *N*-Glycolyl GM3: From Functional Mapping to Novel Anti-ganglioside Specificities

Gertrudis Rojas,^{*,†} Amaury Pupo,[†] Silvia Gómez,[†] Ute Krenzel,[‡] and Ernesto Moreno[†]

[†]Center of Molecular Immunology, Calle 216 esq 15, Atabey, Playa, PO Box 16040, La Habana CP 11600, Cuba

[‡]Department of Chemistry, University of Oslo, PO Box 1033 Blindern, NO-0315 Oslo, Norway

ABSTRACT: The structurally related gangliosides *N*-glycolyl GM3 and *N*-acetyl GM3 are potential targets for tumor immunotherapy. 14F7 is a monoclonal antibody able to discriminate the tumor-specific antigen *N*-glycolyl GM3 from the closely related *N*-acetyl GM3 on the basis of the presence of a single additional hydroxyl group in the former. A combinatorial phage display strategy, based on the screening of a large library followed by refined mutagenesis, allowed a thorough exploration of the binding chemistry of this unique antibody. Three essential features of the heavy chain variable region were identified: two aromatic rings (in positions 33 and 100D) contributing to the binding site architecture and an arginine residue (position 98) critical for recognition. Directed evolution of 14F7 resulted in novel variants that cross-react with the tumor-associated antigen *N*-acetyl GM3 and display recurrent replacements: the substitution W33Q and the appearance of additional arginine residues at several positions of CDR H1. Successful conversion of such engineered variable regions into whole cross-reactive anti-GM3 immunoglobulins validated our phage-based approach to study and modify the lead antibody 14F7. The resulting family of closely related antibodies offers new tools to study the mechanisms of cell death induced by antibodies targeting gangliosides. *In vitro* directed evolution was useful to overcome the technical limitations to obtain anti-ganglioside antibodies. The case of 14F7 illustrates the power of combining library screening with focused site-directed randomization for a comprehensive scanning of protein interactions.



Gangliosides are sialic acid-containing glycosphingolipids prominently present in plasma membranes and involved in cell adhesion, signal transduction, development, differentiation, and tumor progression.¹ Generation of anti-ganglioside antibodies through hybridoma technology has been technically challenging due to the frequent isolation of rather low affinity and broad specificity IgM antibodies recognizing several structurally related glycolipids and other compounds.^{2–5}

14F7 is unique among anti-ganglioside monoclonal antibodies (mAbs). This antibody is produced by a hybridoma derived from a mouse immunized with the ganglioside *N*-glycolyl GM3 conjugated to human very low density lipoproteins.⁶ 14F7 belongs to the IgG1 isotype and recognizes the tumor-specific *N*-glycolyl GM3 ganglioside with high affinity ($K_D = 25 \text{ nmol L}^{-1}$)⁷ and exquisite specificity, being able to discriminate between this target and the closely related *N*-acetyl GM3. The latter ganglioside is widely expressed throughout the body, but overexpressed in several tumors.⁸ The two gangliosides differ from each other only in the presence of a single oxygen atom in the context of a trisaccharide, with *N*-glycolyl GM3 featuring a hydroxymethyl group in place of the methyl group present in *N*-acetyl GM3 (Figure 1). This makes 14F7 an interesting molecule from a chemical point of view, and such interest is reinforced by the biological properties of the antibody. 14F7 binding causes disruption of the tumor cell membrane

integrity,⁹ resulting in anti-tumor activity both *in vitro* and *in vivo*.¹⁰

There is significant interest in the GM3 ganglioside as a target for cancer immunotherapy. This interest is not limited to the tumor-specific *N*-glycolylated form of the ganglioside, as the common *N*-acetylated variant is a tumor-associated therapeutic target in its own right. For example, the anti-GM3 antibody L6D12, an IgM secreted by a transformed human B cell line, was shown to bind several human tumors, without recognizing normal tissues, due to a different GM3 density on normal *versus* cancer cells.¹¹ This antibody was able to induce a complete clinical response in some metastatic melanoma patients.¹² Recombinant hexameric molecules derived from L6D12 have been used to increase its anti-tumor potential.¹³ The search for new anti-GM3 antibodies with better anti-tumor activities has continued. An attempt to circumvent the limitations imposed by the intrinsic immunogenicity of glycolipids, through *in vitro* isolation of anti-GM3 antibody fragments from a human library, rendered moderate and low affinity binders (dissociation equilibrium constants in the micromolar range and even higher) with variable cross-reactivity profiles.¹⁴

Received: July 19, 2012

Accepted: November 8, 2012

Published: November 8, 2012

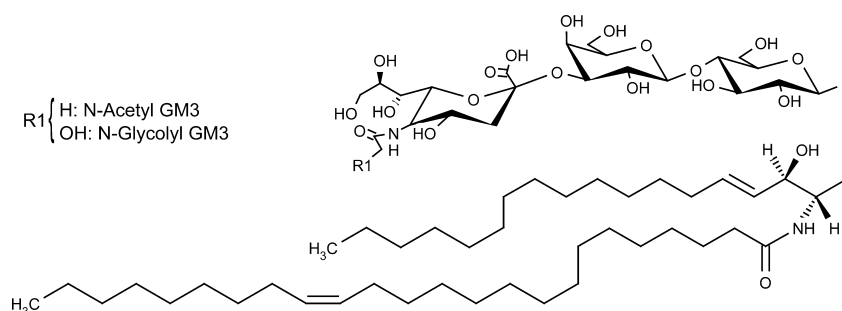


Figure 1. Schematic representation of GM3 variants. *N*-Glycolyl GM3 (NeuGca2-3Gal β 1-4Glc β -Cer(d18:1/24:1(15Z))) and *N*-acetyl GM3 (NeuAca2-3Gal β 1-4Glc β -Cer(d18:1/24:1(15Z))) are distinguished by the presence of either OH or H at R1.

Table 1. Divergence from the Original Sequence at V_H CDR Positions in the Library and among Selected Variants

CDR	Targeted residue	Divergence index (DI) ^a			
		unselected phage-displayed negative variants ^b	positive variants selected on the nominal Ag <i>N</i> -glycolyl GM3 ^c	variants selected on 4G9 mAb also recognizing <i>N</i> -glycolyl GM3 ^d	cross-reactive variants selected on <i>N</i> -acetyl GM3 ^e
H1	Ser 28	17.2	6.2	8.3	7.4
	Phe 29	7.6	1	1	2.1
	Thr 30	10.8	6.5	4.7	6.8
	Ser 31	14.3	6.5	5.9	13
	Trp 33	14.8	1	1	22.2
	Ile 34	4.8	2.1	2.1	2.1
H2	Tyr 50	9.5	3.5	4.2	3.7
	Ile 51	4.5	2.2	3.7	3.5
	Asp 52	9.5	2.1 (Asn*)	2.5 (Asn*)	3.12
	Ala 53	10.6	2.1 (Gly*)	1	3.7
	Thr 54	8.7	6.2	7.1	5.2
	Tyr 56	10.3	9.2	7.8	9.4
	Glu 58	8.7	6.6	1	3.3
H3	Arg 98	11.8	1	1	1
	Leu 99	5.8	3.6	2.8	4.9
	Arg 100	16.7	2.1	1	1
	Arg 100A	10.3	2.1	5.9	1
	Gly 100B	7.5	4.4	1	1
	Ile 100C	8.1	4.4	1	3.7
	Tyr 100D	11.4	2.1 (Phe*)	1	1

^aDI values reflect the divergence of a group of sequences from the original V_H at each position and were calculated as follows: DI = number of different residues at a given position/frequency of the original residue. ^bUnselected clones from the soft randomization library ($n = 50$) were shown to produce phages displaying antibody fragments as assessed by ELISA with the anti-*c-myc* tag antibody. None of them was able to bind *N*-glycolyl GM3. ^cA group of clones (having 36 unique V_H protein sequences) retrieved after a single panning round on *N*-glycolyl GM3 produced phage-displayed antibody fragments recognizing this Ag by ELISA. ^dA second group of clones (25 unique sequences) was selected in two rounds by the anti-idiotypic antibody 4G9. All of them produced phage-displayed antibody fragments retaining reactivity to the nominal Ag *N*-glycolyl GM3. ^eCross-reactive phage-displayed antibody fragments (22 unique sequences) recognizing both *N*-glycolyl and *N*-acetyl GM3 were retrieved after three selection rounds on the second ganglioside. Positions with low divergence indexes (<3) are highlighted in gray. *In some positions with low divergence indexes, the single additional tolerated residue (between parentheses) shares features such as size, shape, or chemical properties with the original one.

In this context, the properties of 14F7 offer a unique opportunity to understand and manipulate anti-ganglioside antibodies. The aims of the current work were hence to identify

the critical residues within heavy chain variable region contributing to the exquisite 14F7 specificity and to use 14F7 as a lead molecule to obtain a family of anti-GM3 antibodies

that recognize both GM3 forms, overcoming through *in vitro* molecular evolution the biological barriers that hamper the generation of antibodies against glycolipids.

RESULTS AND DISCUSSION

We developed an efficient combinatorial strategy to target the 14F7 binding site, based on previous structural knowledge¹⁵ and phage display⁷ studies, which was used to obtain a functional map of the 14F7 paratope and to generate novel variants that cross-react with the closely related *N*-acetyl GM3 ganglioside.

Controlled Diversification of V_H CDRs of Phage-Displayed 14F7 Antibody Fragment Resulted in a Library of Variants with Different Ag-Binding Properties. The previously obtained 3Fm phage-displayed single chain Fv antibody fragment (scFv),⁷ combining the original 14F7 heavy chain variable region (V_H) with a surrogate light chain variable region (V_L), served as the scaffold for library construction. The surrogate light chain was not changed in the library, due to the observed association of ganglioside binding with V_H.^{7,15} Knowledge of the 14F7 Fab crystal structure¹⁵ allowed a rational library design targeting 20 residues located within the three V_H complementarity-determining regions (CDR H1, CDR H2, and CDR H3) (Table 1). Most of these positions, having solvent-exposed side chains, were soft randomized, meaning that the introduction of a diverse mixture of amino acids (aa) at each targeted position was always biased toward the predominance of the residue present in the original 3Fm scFv. The probability of keeping the original nucleotide at each targeted DNA position was set to 85% during gene library synthesis, resulting in most library members displaying the original residue at a given position.

Some positions were not randomized but substituted by small sets of residues, always biased toward the original aa. For example, F29, I34, and I51 were replaced only by three or four additional hydrophobic aa, taking into account their well-established structural roles.¹⁶ The same was done to replace L99, which packs against the aromatic ring of Y100E at the base of the CDR H3. D52, previously proposed to be at the core of the binding site¹⁵ on the basis of modeling and mutagenesis studies, was substituted by a reduced set including six additional aa (predominantly small and medium sized residues). Other CDR positions were not mutated at all due to their likely involvement in V_H folding, maintenance of CDR canonical conformations, or in shaping the base of the CDR H3 loop.

Phage enzyme-linked immunosorbent assay (ELISA) screening of 160 randomly taken clones from the library did not yield any binder to either *N*-glycolyl GM3 or the control antigen (Ag) *N*-acetyl GM3, showing that our soft randomization approach resulted in a drastic modification of the binding properties for most of the library members. Nevertheless, one phage selection round on immobilized *N*-glycolyl GM3 was enough to pick phage-displayed antibody fragments recognizing this antigen. No additional selection rounds were performed in order to study a vast diversity of such positive clones without any bias introduced by repeated phage amplification cycles.

Phage Selection on the Nominal Antigen *N*-Glycolyl GM3 Revealed Key Features Associated with Ag Recognition. Selection on *N*-glycolyl GM3 resulted in an enrichment of the phage pool in less mutated variants from the library (Figure 2). While the majority of unselected, Ag-binding negative, antibody fragments had five or six aa changes as compared to the original scFv, most of the selected variants

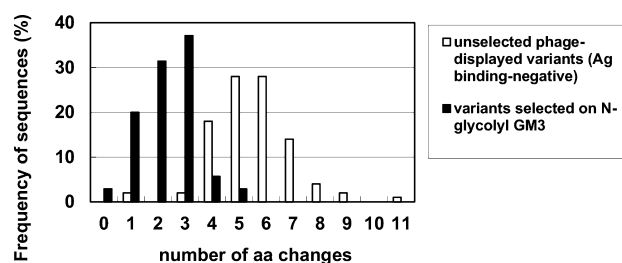


Figure 2. Selection of sequences closer to the original 14F7 V_H after phage selection on the nominal Ag *N*-glycolyl GM3. V_H amino acid sequence identity compared to the original V_H was assessed in samples of unselected phage-displayed Ag-binding negative antibody fragments (50 unique sequences) from the library, and positive variants (36 unique sequences) picked after one selection round on immobilized *N*-glycolyl GM3. Ag recognition was evaluated by phage ELISA on *N*-glycolyl GM3-coated plates. Phage display of all antibody fragments was confirmed by ELISA on plates coated with the anti-tag 9E10 antibody (recognizing the *c-myc* tag fused to the C-terminus of antibody fragments in our display system). Frequencies were calculated as the ratio between the amount of unique V_H sequences within a group of variants (either unselected or selected) that display a given number of aa replacements (as compared with the original V_H) and the total amount of unique sequences within the same group.

showed only two or three mutations. Confirmation of successful phage display of antibody fragments with the anti-tag antibody 9E10 (recognizing the *c-myc* tag fused to the C-terminus of the antibody fragments in our display system) was a prerequisite to include the non-binders in the comparison, in order to focus the analysis on Ag recognition, without the interference of newly introduced stop codons and other sequence changes impairing protein display.

We introduced a divergence index (DI) to predict the relative contribution of the individual residues to Ag binding (Table 1). DI within a group of variants with defined binding properties was calculated for each position according to eq 1:

$$DI = \frac{\text{no. of different residues at the position}}{\text{frequency of the original residue}} \quad (1)$$

The frequency of the original residue was calculated as the ratio of the number of unique sequences having the original residue (within a group of variants) relative to the total number of unique sequences in this group. Phage-displayed variants retrieved from the library were classified in four groups: unselected, selected on *N*-glycolyl GM3, selected on the 4G9 anti-idiotypic mAb¹⁷ (and also recognizing *N*-glycolyl GM3), and selected on the closely related ganglioside *N*-acetyl GM3 (keeping reactivity with *N*-glycolyl GM3).

We envisage DI as a valuable tool to analyze the results of antibody directed evolution. This approach is related, although not identical, to the use of Kabat's variability indexes,¹⁸ which have been very useful for studying antibody repertoires.

The DI values among unselected Ag-binding negative phage-displayed variants, ranging from 4 to 18, reflected the actual library diversity. The divergence from the original sequence at some positions strongly decreased under the Ag-driven selective pressure (Table 1), suggesting a role for the corresponding residues in recognition. F29, W33, and R98 were absolutely conserved among the variants recognizing *N*-glycolyl GM3 (DI = 1), whereas I34, I51, D52, A53, R100, R100A, and Y100D were partially conserved (DI < 3). The remaining targeted positions showed higher DI values and

Table 2. V_H Sequences of the Antibody Fragments Cross-Reactive to *N*-Acetyl GM3^a

Representative clone	CDR H1	CDR H2	CDR H3	Frequency
Original 14F7 scFv	26	35 50 52A	65 95 100A 101	-
(<i>N</i> -glycolyl GM3-specific)				
	GYSFTSYWIH	YIDPATAYTESNQKFKD	ESPLRRGIYYYYAMDY	
CR1	-- R -- Q --	-----	-----	28/54
CR2	---- R -- Q --	--N---S-----	-----	1/54
CR3	-- R -- NQ --	F-----	-----	1/54
CR4	---- NR -- Q --	D---GR-----	-----	1/54
CR5	---- RR -- Q --	-----N-----	-----	1/54
CR6	--- I -- R -- Q --	--N---S-----	---F-----	1/54
CR7	---- K -- Q --	F-N-----	-----	1/54
CR8	---- R -- Q --	-----N-----	-----	1/54
CR9	---- R -- Q --	F---S---V-----	-----	2/54
CR10	---- Q --	--N---S-----	-----	2/54
CR11	---- R -- Q --	-----K-----	-----	2/54
CR12	---- R -- Q --	-----	-----R-----	1/54
CR13	---- R -- Q --	--N-GS-----	---M-----	2/54
CR14	-- R -- R ---	-L---N-----	---V-----	1/54
CR15	-- R -- R ---	-V---N-----	---V-----	1/54
CR16	---- R -- Q --	--N-----	-----	2/54
CR17	--- NR -- Q --	-----W-----	-----	1/54
CR18	-- T -- R -- Q --	---G-----	-----	1/54
CR19	-- P -- R -- Q --	---R-----	-----L-----	1/54
CR20	--- SR -- QV ---	-V---H-----	-----L-----	1/54
CR21	-- H --- Q --	--N-----	-----	1/54
CR22	---- R -- Q --	--N---D-----	-----L-----	1/54

^aA total of 54 clones able to produce phages recognizing both *N*-glycolyl and *N*-acetyl GM3 were identified by ELISA screening after three selection rounds from 14F7-derived phage library on immobilized *N*-acetyl GM3. Sequencing the corresponding scFv genes revealed 22 unique deduced protein sequences (CR variants) among them, each one represented one or several times. CDR residues different from the ones in the original 14F7-derived scFv are shown. Lines indicate conservation of the original amino acid. Non-CDR sequences were totally conserved. Recurrent mutations in CDR H1 (W33Q and newly appearing Arg residues) are shown in bold.

accommodated diverse residues while retaining recognition of the nominal Ag.

The conserved residues among positive variants delineated a functional map of the Ag binding site. Several of them play structural roles in V_H folding and exhibited limited diversity even in the initial library (F29, I34, and I51), whereas the conservation of the rest could be related to *N*-glycolyl GM3 recognition.

In a parallel experiment, phage selection from the library was performed on the immobilized anti-idiotypic antibody 4G9. This monoclonal IgG1 antibody is produced by a hybridoma derived from a mouse immunized with 14F7 mAb and was shown to recognize specifically the 14F7 paratope.¹⁷ The use of 4G9 as a selector molecule provided an independent set of variants that, although evolved under a different selective pressure, were all reactive to *N*-glycolyl GM3 (Table 1). The analysis of this second group reinforced the interest on most of the residues previously highlighted through *N*-glycolyl GM3-driven selection (F29, W33, I34, D52, A53, R98, R100, and Y100D), which were again conserved.

Several combinatorial approaches have been used to study the binding chemistry of antibodies.^{19,20} While total CDR randomization¹⁹ implies the risk of retrieving totally new binding sites with different Ag-binding modes, our soft randomization strategy allowed us to focus on a relatively narrow sequence space surrounding the original 14F7 binding site. As compared to alanine/homologue scanning,²⁰ the

involvement of multiple residues (theoretically any) in soft randomization can shed more light on the interactions.

Cross-Reactive Phage-Displayed Variants with Recurrent CDR H1 Changes Were Selected on the Closely Related *N*-Acetyl GM3 Ganglioside. Contrasting with the quick selection on the nominal Ag, three panning rounds on immobilized *N*-acetyl GM3 were required to isolate positive variants. All of them retained reactivity to *N*-glycolyl GM3, reflecting cross-reactivity to a closely related Ag rather than a switch in specificity. The sequence divergence pattern among cross-reactive variants was overall similar to that exhibited by the antibody fragments keeping the original reactivity (Table 1), except for CDR H1, which was remarkably modified, including the frequent substitution W33Q and the emergence of one or more Arg residues at various positions (Table 2). Most cross-reactive antibody fragments had several such changes.

A parallel protocol included depletion on immobilized *N*-glycolyl GM3 before each selection round on *N*-acetyl GM3, in order to segregate the reactivity toward each GM3 variant. No positive binders could be picked up until the fourth round, after which again only cross-reactive variants were retrieved, probably due to a minor depletion escape and a slow enrichment. All of the variants, including the predominantly selected triple-mutated one, had been previously obtained without depletion. The latter procedure only delayed enrichment, indicating the absence of variants with a true specificity switch among the library members.

In addition to the above-described CDR H1 substitutions, most of the cross-reactive variants (except for the predominant one) exhibited one or more additional changes. In order to define the precise molecular bases underlying the cross-reactivity emergence, new variants having only the recurrent CDR H1 changes were constructed and characterized (Figure 3, panel a). The three variants having the most frequently

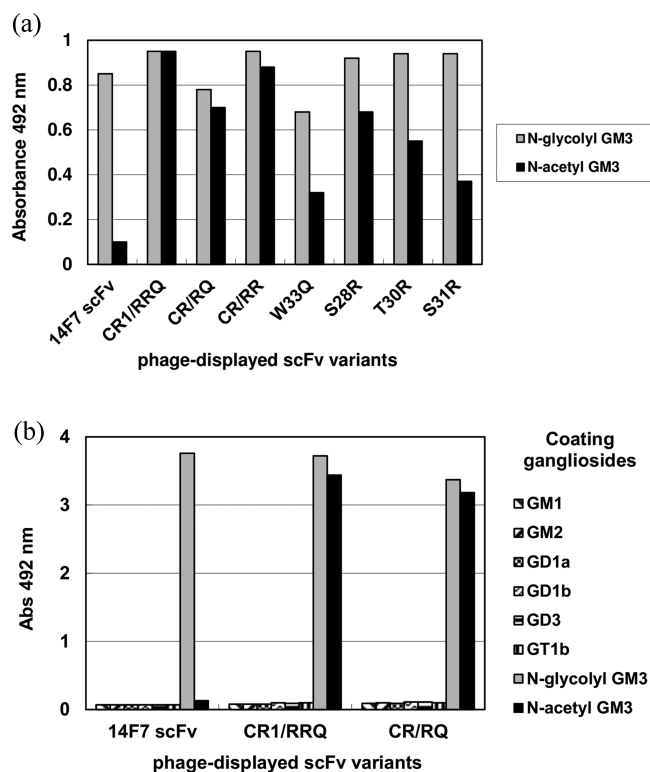


Figure 3. Recognition profiles of novel antibody fragments cross-reactive to *N*-acetyl GM3. Phage samples were incubated on polyvinyl chloride microplates coated with gangliosides. Bound phages were detected with an anti-M13 antibody conjugated to horseradish peroxidase. The tested variants were characterized by the presence of either three mutations (S28R + T30R + W33Q in CR1/RRQ), two mutations (S31R + W33Q in CR/RQ and S28R + S31R in CR/RR), or single mutations (W33Q, S28R, T30R, or S31R) at CDR H1. The original 14F7-derived scFv was included as a control. (a) Diluted phage-containing supernatants (10^{10} viral particles mL^{-1}) were used to confirm cross-reactivity of variants with recurrent CDR H1 mutations toward *N*-acetyl GM3. (b) Purified phages (10^{11} viral particles mL^{-1}) from two selected cross-reactive variants were used to evaluate specificity toward a wider panel of gangliosides.

observed combinations of CDR H1 mutations were highly cross-reactive, showing more than 90% reactivity toward *N*-acetyl GM3 as compared to *N*-glycolyl GM3. The most frequent individual substitution (W33Q), found in 20 out of 22 cross-reactive variants, conferred only a moderate cross-reactivity (47%) when introduced alone. S28R, T30R, and S31R resulted in variable levels of partial cross-reactivity (from 74% to 39%). Taken together, these results confirmed the direct contribution of the recurrent CDR H1 changes to extending the specificity toward *N*-acetyl GM3.

The current success to retrieve cross-reactive antibody fragments contrasts with our previous unreported failure to modify phage-displayed 14F7 toward recognition of *N*-acetyl GM3 through individual mutagenesis. These attempts were

based on the rather intuitive idea of creating a hydrophobic pocket able to accommodate the methyl group. In contrast to our expectations, replacements arising from the library under the selective pressure of *N*-acetyl GM3 involved polar residues (Gln and Arg). While rational design often requires defining a limited search space in order to obtain a testable number of solutions, 14F7 directed evolution highlights the usefulness of exploring a larger sequence space, in order to underscore unexpected structural solutions for complex molecular interactions. Similar approaches have been used to target different members within families of structurally related antigens, such as steroids²¹ and sulfonamides,²² starting with a lead antibody that recognizes one of them.

Cross-Reactivity with *N*-Acetyl GM3 Was Not Due to Nonspecific Polyreactivity. The gain of recognition toward *N*-acetyl GM3 reflected specific cross-reactivity to a closely related ganglioside, not relying on promiscuous interactions that would result in nonspecific polyreactivity. This was shown with a panel of diverse gangliosides, none of which was recognized by the new cross-reactive variants (Figure 3, panel b).

Mutations Identified in Phage-Displayed Variants Conferred a Similar Cross-Reactivity to the Whole Immunoglobulin. The phage-displayed 14F7-derived scFv, although resembling the binding properties of the original mAb,⁷ exhibits structural differences as compared to the antibody. The scFv construction implies the absence of the constant domains and the introduction of a 16 aa linker to connect V_H and V_L . Furthermore, a surrogate V_L with low sequence identity to the original 14F7 V_L (60%) was used in order to achieve phage display.⁷

While the phage-displayed format allowed an extensive screening of multiple changes of the 14F7 binding site, the final goal was to recapitulate the specificity change in whole antibodies, which could be directly compared with 14F7. New recombinant immunoglobulins, including two different sets of CDR H1 mutations, were constructed and shown to resemble the immunochemical properties of the phage-displayed cross-reactive variants (Figure 4). The remaining aa sequence of both molecules was identical to that of the reported chimeric (mouse/human) version of 14F7,⁹ including the original V_L .

We were able to close the circle from an antibody with relevant biological properties to novel antibodies ready to be characterized in a similar biological setting. While the intermediate steps involved design, construction, and *in vitro* evolution of engineered scFv antibody fragments, the fact that the selected mutations conferred the desired binding properties to whole recombinant immunoglobulins validates our phage-based approach to manipulate the 14F7 binding site and gives us the tools to go back to our original field of interest: targeting gangliosides for tumor immunotherapy.

The availability of closely related antibodies (14F7 and the cross-reactive variants) with different recognition patterns toward two antigens that are closely related as well offers a unique opportunity for a thorough exploration of the cytotoxic effects mediated by anti-ganglioside antibodies. Experiments showing that the new cross-reactive mutated antibodies keep the ability to kill *N*-glycolyl GM3-positive cells and also acquire cytotoxic activity against cells lacking expression of *N*-glycolyl GM3, but *N*-acetyl GM3-positive, provided the proof of principle of their usefulness as tools to study cell death (A. V. Casadesus, Center of Molecular Immunology, personal

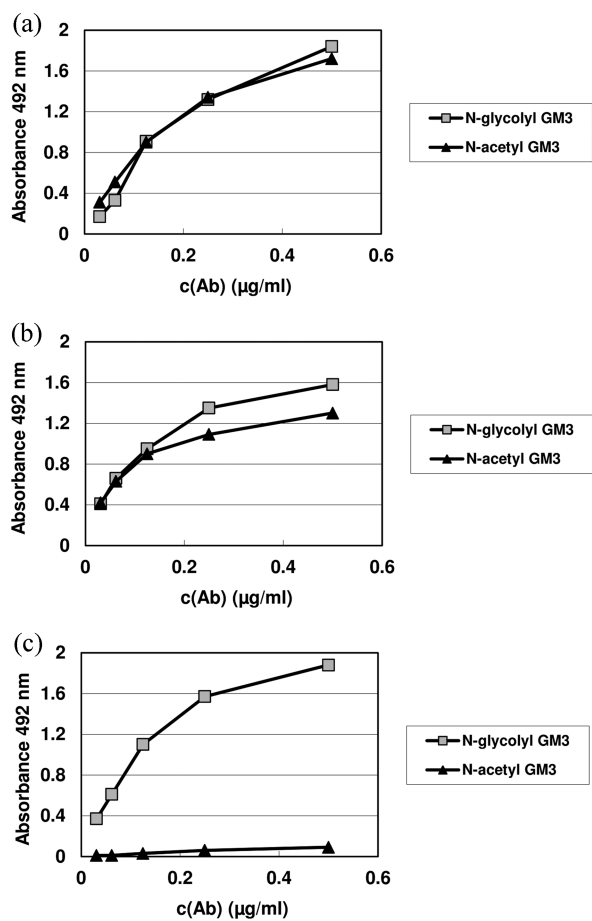


Figure 4. Cross-reactivity of 14F7-derived whole recombinant immunoglobulins. Chimeric versions of 14F7 including either three mutations (a) (S28R + T30R + W33Q in CR1/RRQ) or two mutations (b) (S31R + W33Q in CR/RQ) at CDR H1 were tested on polyvinyl chloride microplates coated with either *N*-glycolyl or *N*-acetyl GM3. Chimeric 14F7 was included as a control (c). Bound antibodies (Ab) were detected with an anti-human IgG antibody conjugated to horseradish peroxidase.

communication). They could be used to individually target each ganglioside on cells such as B16 melanoma and P3 X63 Ag8.653 myeloma, which have a strong predominance of *N*-acetyl²³ and *N*-glycolyl GM3,²⁴ respectively.^{25,10}

A Refined Functional Map of the Ag Binding Site Was Delineated by Assessing the Contribution of Individual Residues. Library screening defined general molecular rules of recognition, but the presence of several mutations in most of the library members precluded the assessment of the individual role of any particular residue. For example, the loss of Ag recognition might be the net result of several changes, each having only a minor detrimental influence, while compensatory mutations could mask the effect of changing an actually critical residue. On the other hand, the binding contribution of some residues might be overestimated in a suboptimal context, where other changes tend to decrease recognition.

In order to delineate the detailed molecular determinants of *N*-glycolyl GM3 binding by 14F7, we randomized individual positions of the original 3Fm scFv (Table 3) that were conserved among positive variants from the library. F29, I34, and I51 were excluded because their conservation is most likely associated with a structural role rather than with Ag binding. R100 and R100A were relatively conserved, and all of the Ag-

binding variants kept at least one of them. Since these data suggested that at least one of these neighboring Arg residues is necessary for Ag binding, their codons were randomized simultaneously.

Confirmation of successful phage display of the new variants with the anti-*c-myc* tag antibody was required to include them in the analysis, in order to avoid confusing effects of mutations affecting protein display rather than Ag recognition. Substitutions by Cys and Pro were analyzed with particular caution, because even when such variants were displayed, they could have severe folding disturbances.

Detailed analysis of the tolerated/non-tolerated mutations (Table 3) confirmed the critical role played by three residues (W33, R98, and Y100D) for the specific recognition of *N*-glycolyl GM3. Substitution of either W33 or Y100D by multiple aa abolished binding. The original reactivity was preserved when such positions were occupied by two other aromatic residues. This is consistent with the fact that the aromatic rings of both W33 and Y100D are almost completely buried, presumably playing a role in shaping the conformation of the CDR H3 loop, which may be altered by mutations targeting these critical positions.

Strikingly, the only tolerated non-aromatic residue at position 33 was Gln, compatible with *N*-glycolyl GM3 recognition, but resulting in a moderate cross-reactivity to *N*-acetyl GM3, as described above. The effect of changing R98 was even more dramatic. All characterized substitutions at this position, including the conservative substitution by Lys, totally abolished Ag binding.

D52 could be replaced by Asn and by the only other acidic residue, Glu, as well as by several small aa, whereas other residues, including those with bulky side chains, precluded Ag recognition. Mixed effects of D52 targeting suggest that this residue (although not absolutely required for binding) is in close proximity to the bound Ag.

While both R100 and R100A could be substituted by a number of residues, even simultaneously, we found a predominance of combinations that retained one Arg or exhibited another basic residue instead (Lys/His) among the variants recognizing *N*-glycolyl GM3. On the other hand, combinations including a negatively charged residue resulted in the loss of Ag recognition, and the same happened with two combinations including Cys or exhibiting Pro at position 100. At least one of the two positions required a polar residue, preferably with a positive charge. These results are consistent with a contribution of R100/R100A to ganglioside binding.

No single substitution targeting A53 affected recognition, except for the replacement by Cys, which could cause folding disturbances and aggregation mediated by undesired intra- and intermolecular disulfide bridges.

A functional map of the paratope, based on the sequence divergence profiles among Ag-binding variants and refined through focused site-directed mutagenesis, is shown in Figure 5a.

The Functional Map of a Novel Cross-Reactive Binding Site Was Found to Overlap with the Original 14F7 Map. A question arising from the emergence of new variants with extended specificity toward *N*-acetyl GM3 is to what extent ganglioside binding by such modified paratopes resembles the original interaction between 14F7 and the nominal Ag. In order to address this question, a detailed functional map of one of the cross-reactive binding sites (CR1/RRQ) was defined. While keeping its mutated CDR H1

Table 3. Effects of Substitutions Introduced by Site-Directed Mutagenesis on Binding Properties

Targeted residue	Antibody fragments specific to <i>N</i> -glycolyl GM3 (derived from the original 3Fm scFv)		Antibody fragments recognizing both <i>N</i> -glycolyl and <i>N</i> -acetyl GM3 (derived from the CR1/RRQ cross-reactive variant)	
	Tolerated substitutions	Mutations abolishing binding	Tolerated substitutions	Mutations abolishing binding
Trp 33	F, Y, Q*	C, E, G, H, K, N, P, R, S, T	Not assayed	Not assayed
Asp 52	A, E, N, S, T	C, F, H, K, P, R, V, Y	A, E, N, S, T	G, C, P, R
Ala 53	E, F, G, H, I, L, N, V	C	D, E, G, H, L, S, T, Y	-
Arg 98	-	A, E, G, I, K, L, M, Q, S, T, V, W, Y	-	E, G, I, K, M, N, P, Q, S, T, V, W
Arg 100-Arg 100A	KS, QP, RI, RL, RQ, RW, SP, TK, TQ, YH	GC, LD, PA, TD	AK, HR, TR	AL, DR, LS, PQ, PT, TP, WP
Gly 100B	Not assayed	Not assayed	A, D, F, L, Q, R, S	C
Tyr 100D	F, W	D, H, K, L, Q, R, S, T, V	F	D, G, H, K, L, P, R, S, T, V

*Substitution maintaining recognition of *N*-glycolyl GM3 and producing moderate cross-reactivity to *N*-acetyl GM3.

Selected positions were randomized by Kunkel mutagenesis with degenerate oligonucleotides on the original 14F7-derived scFv and the cross-reactive CR1/RRQ variant. Mutated variants, either retaining their ability to recognize the corresponding antigen(s) or unable to bind any antigen despite being successfully displayed (as assessed with the anti-*c-myc* tag antibody), were identified by phage ELISA on ganglioside-coated microplates. The corresponding phagemid inserts were sequenced and protein sequences were deduced.

unchanged, other positions that were highly conserved among cross-reactive variants (Table 1) were randomized to assess their individual contribution to binding.

The resulting sets of tolerated/non-tolerated substitutions closely resembled those defined through targeting of the 14F7 paratope (Table 3). The critical role of residues at positions 98 and 100D and the mixed effects of substituting D52 had been already observed for the original 14F7-derived scFv. A marked preference for sequences having a basic residue at position 100A and non-negative amino acids at position 100 was found. The cross-reactive variant appears to be more sensitive to changes at these positions than the original 3Fm scFv. Functional mapping of the cross-reactive paratope (Figure 5b) did not reveal any drastic differences as compared to the original binding site, indicating that ganglioside binding by both is very similar.

Revisiting Our Understanding of the Binding Chemistry of 14F7. While a library of single substituted molecules would be ideal to define the exact contribution of each residue to binding,²⁶ our dual purpose library (composed mainly of molecules with multiple substitutions) was useful to delineate a general picture of recognition and also to underscore the complex combinations of substitutions required for cross-reactivity to evolve. Closer examination of selected residues by site-directed randomization refined the functional map, allowing a comprehensive scanning of the interactions.

The previously proposed model of 14F7-ganglioside interaction¹⁵ is not fully compatible with the current mutagenesis data. The polar groups of W33, D52, and Y50 (predicted to form a hydrophilic pocket able to accommodate the hydroxyl group of the glycolyl moiety) are not critically required for recognition. Furthermore, the extension of specificity toward *N*-acetyl GM3 mediated by W33Q is not explained by the model, since the hydrophilic pocket described above is even reinforced by the polar Gln amide.

The current study identified three positions as critical for Ag binding: 33, 98, and 100D. R98 is strictly conserved among Ag-binding variants, which is consistent with the well documented role basic aa have in the recognition of negatively charged carbohydrates.²⁷ The presence of three Arg residues in the 14F7 CDR H3 has been interpreted as an important determinant of ganglioside recognition, and it was indeed possible to increase the affinity of another antibody recognizing *N*-glycosylated gangliosides through the introduction of a third Arg residue in its CDR H3.²⁸ Our results show a clear hierarchy in the role of the different Arg residues, with R98 being the only one of critical importance. The presence of two aromatic rings in positions 33 and 100D is likely to be related to the establishment of π - π stacking interactions between them, contributing to the stability of the binding site architecture.

The most intriguing finding from the directed evolution experiments is the emergence of the substitution W33Q (compatible with *N*-glycolyl GM3 recognition). Gln was hence

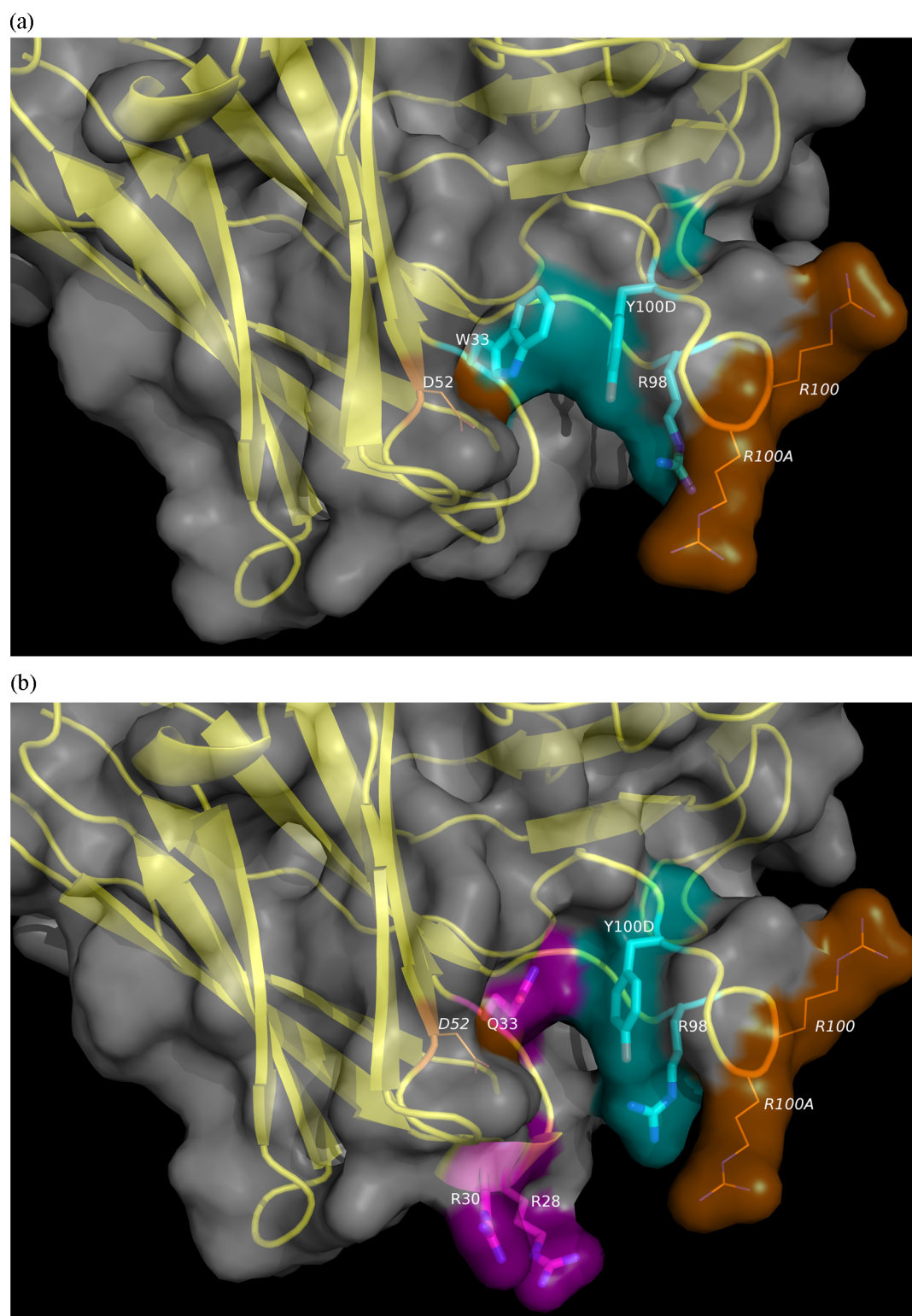


Figure 5. (a) Representation of the functional 14F7 paratope as defined by mutagenesis experiments. 14F7 Fv is represented as a cartoon with gray surface (based on the mouse 14F7 Fab crystal structure, PDB entry 1RIH). Residues occupying positions critical for *N*-glycolyl GM3 recognition are shown in cyan (side chains are represented as sticks). Residues proposed to be close to the ligand and/or contributing to binding, but not critically required for recognition, are shown in orange with side chains represented as lines. The figure was generated with Pymol. (b) Representation of the functional paratope of a cross-reactive variant recognizing both *N*-glycolyl and *N*-acetyl GM3. Residues in positions that are critical for the recognition of both Ags, as well as additional residues proposed to be close to the bound Ags, are represented as in panel a. The substitutions S28R, T30R, and W33Q were introduced in the 14F7 Fv structure with Pymol. These newly introduced residues, which contribute directly to cross-reactivity, are shown in magenta, with side chains represented as sticks.

the only non-aromatic residue able to occupy a position presumed to be involved in aromatic π - π stacking interactions. It is possible that Gln engages in amino- π interactions^{29,30} between its partially charged amide $N\epsilon$ and the aromatic ring of Y100D, stabilizing the binding site conformation in a similar way as the original interaction between W33 and Y100D. In this context, it is worth noting that, in its most likely rotamer, the Gln side chain superimposes well on the pyrrole ring of Trp. This would place a hydrogen-donor group in almost the same position as before. The Gln $N\epsilon$ group is a potential hydrogen-donor for two H-bonds, whereas Trp can engage in only one such interaction. In addition, the Gln amide oxygen may serve as H-bond acceptor. Gln can thus provide additional interactions as compared to Trp, while maintaining the paratope architecture, and this could explain the (moderate) cross-reactivity associated with W33Q replacement.

Cross-reactivity was strongly enhanced by the simultaneous presence of Arg residues in CDR H1. Arg is a major functional contributor to protein interfaces arising from directed evolution, due to its potential to establish electrostatic interactions and hydrogen-bonding.³¹ Arg residues could act primarily to attract negatively charged gangliosides allowing subsequent accommodation into the binding site. Alternatively, it is also possible that Arg was selected due to its combination of hydrophobic and hydrophilic side chain properties, which could result in the binding of molecules with amphipathic properties, such as *N*-acetylGM3.

While docking simulations and further mutagenesis experiments are currently ongoing in order to obtain a model of the interaction that turns out to be compatible with the data arising from this extensive mutagenesis study, only experimental structural studies of the complexes between 14F7 (and its derivatives) and gangliosides will reveal the precise interaction modes.

Concluding Remarks. The case of 14F7 illustrates the power of phage display to provide new insights into the chemistry of binding sites and to reveal structural solutions difficult to predict in order to modulate antibody specificity. The strategy of combining large library screening with focused site-directed randomization allows a comprehensive scanning of the interactions and could be applied to other problems related to the chemical basis of biological phenomena. The novel anti-GM3 cross-reactive antibodies are valuable tools to explore the role of different gangliosides in the complex interplay between tumors and the immune system.

METHODS

Library Construction. The V_H gene library was designed as follows. Codons coding for F29, I34, I51, and L99 were substituted by TTT, ATT, ATT, and TTG, respectively. Underlined letters represent the mixture of the mentioned nucleotide (85%) plus the equimolar combination of the remaining three nucleotides (15%). Such partially degenerate codons coded for small sets of hydrophobic aa, enriched in the original ones. DS2-coding codon was substituted by the unique triplet (80% G/20% A)A(50% C/50% T), able to code for a mixture of seven aa, rich in the original Asp. The remaining 15 targeted residues at V_H CDRs (Table 1) were soft randomized with degenerate triplets containing the original nucleotide (85%) plus the equimolar mixture of the three remaining nucleotides (15%) at each position.

GENEART (Germany) synthesized and cloned the V_H gene library into the 3Fm scFv scaffold⁷ contained within the pHAB phagemid vector, according to our design, and transformed *E. coli* TG1 ((K12 (*lac-pro*), *supE*, *thi*, *hsdD5/F'* *traD36*, *proA*⁺*B*⁺, *lacI*^q, *lacZ*_{M15}) cells to create a library of 3×10^8 members. pHAB

phagemid includes the lac Z promoter, the gene coding for the M13 PIII signal peptide, suitable restriction sites for cloning V_H and V_L genes, the genes coding for hexahistidine and *c-myc* tags (followed by an amber stop codon), the M13 gene 3, and an ampicillin resistance gene. V_H gene precedes V_L gene in these constructs, and both are connected by the DNA sequence coding for a linker (APQAKSSSGSGSESKVD). The 3Fm scFv scaffold contains, besides the elements described above, an invariant mouse V_L gene.⁷

Phage Selection. *N*-Glycolyl or *N*-acetyl GM3 (10 μg /well in methanol) were dried on 6-well tissue culture plates. Alternatively, immunotubes were coated overnight at 4 °C with the anti-idiotypic 4G9 mAb that recognizes 14F7 paratope at 10 $\mu\text{g mL}^{-1}$ in phosphate buffered saline (PBS). Purified phages rescued from the library with M13 KO7 helper phage as described³² (5×10^{12} viral particles) and coated wells/immunotubes were blocked with PBS containing 2% (w/v) skim powder milk (M-PBS) for 1 h at RT. Blocked phages were incubated on blocked wells/immunotubes for 1 h at RT. Wells/tubes were washed 20 times with PBS containing 0.1% (v/v) Tween 20 (PBS-T) and twice with PBS. Bound phages were eluted with 100 mmol L⁻¹ triethylamine for 10 min at RT and neutralized with 1 mol L⁻¹ Tris, pH 7.5. Selected phages were rescued, purified, and used to start a new selection round. A single selection round on *N*-glycolyl GM3 was carried out, while phage selection procedures on 4G9 mAb and *N*-acetyl GM3 included two and three rounds, respectively.

An independent selection protocol included depletion of blocked phages on *N*-glycolyl GM3-coated and blocked wells for 1 h at RT before each of the four selection rounds on *N*-acetyl GM3-coated wells.

Phage Screening by ELISA. Selected phages were individually rescued in 96-deep-well plates from phagemid-transformed TG1 colonies.³² Polyvinyl chloride microplates containing gangliosides (10 $\mu\text{g mL}^{-1}$ in methanol) were dried. Alternatively, plates were coated overnight at 4 °C with the anti-*c-myc* tag 9E10 mAb at 10 $\mu\text{g mL}^{-1}$ in PBS. Plates were blocked for 1 h at RT with M-PBS. Phage-containing supernatants (diluted 1:5 in M-PBS) or diluted purified phages were added. After 2 h at RT, plates were washed with PBS-T, and an anti-M13 mAb conjugated to horseradish peroxidase (HRP, GE Healthcare, USA), appropriately diluted in M-PBS, was added. Plates were incubated for 1 h at RT and washed. Substrate solution (500 $\mu\text{g mL}^{-1}$ *o*-phenylenediamine and 0.015% (v/v) hydrogen peroxide in 0.1 mol L⁻¹ citrate-phosphate buffer, pH 5.0) was added. After 15 min the reaction was stopped with 2.5 mol L⁻¹ sulfuric acid. Absorbances (Abs) at 492 nm were read. Variants selected for further characterization included those retaining *N*-glycolyl GM3 recognition (showing more than 75% of the original 14F7 scFv reactivity) and those that had lost it (less than 25% of specific reactivity despite a high reactivity with the anti-tag 9E10 mAb), as well as cross-reactive variants recognizing also *N*-acetyl GM3. Selected phagemids were sequenced by Macrogen (Korea).

Construction and Characterization of Recombinant Immunoglobulins. Two mutated V_H genes (from the cross-reactive variants) were synthesized by GENEART (Germany) and cloned into the expression vector pAH4604,³³ containing the gene coding for the human IgG1 constant region. Mouse myeloma Sp2/0 cells were electroporated with these constructs and with previously obtained 14F7 chimeric light chain gene-containing vector pAG4622.⁹ Electroporation was performed at 200 V and 950 μF in PBS using the GenePulser electroporator (BIORAD, USA). Histidinol (10 nmol L⁻¹) was used as the selection drug. Culture supernatants were screened by ELISA (see below), and cells producing antibodies recognizing both gangliosides were cloned twice by limiting dilution.

Polyvinyl chloride microplates were coated with either *N*-glycolyl or *N*-acetyl GM3 and blocked, as described above. Supernatants from transfected cells were diluted in M-PBS (human immunoglobulin concentrations were previously measured by ELISA) and incubated on the plates for 2 h at RT. After washing with PBS-T, anti-human Fc antibodies conjugated to HRP (Sigma, USA), appropriately diluted in M-PBS, were added. Plates were incubated for 1 h at RT and washed again. Color development and absorbance measurement were performed as described above.

Site-Directed Mutagenesis. Selected positions were mutated/randomized by Kunkel mutagenesis,³⁴ using described procedures.³⁵ Single strand DNA (from either the original 3Fm scFv or the cross-reactive variant CR1/RRQ) obtained from phages produced by the CJ236 *E. coli* strain (*duf ung thi-1 relA1 spoT1 mcrA/pCJ105(F' cam^r)*) was used as template. 3Fm template allowed mutagenesis of the original 14F7-derived scFv, while CR1/RRQ template included three mutations that result in cross-reactivity of the corresponding antibody fragment with *N*-acetyl GM3 and was used to study the effect of mutations on the cross-reactive binding site. Antisense mutagenic oligonucleotides included 15 nucleotides complementary to the template at each end, flanking the target region that contained one or more triplets to be replaced. The desired mutations were directly introduced into the oligonucleotides. Randomization was accomplished by inserting the degenerate sequence NNK. New variants (40 clones from each randomization reaction) were screened by phage ELISA and sequenced as described above.

AUTHOR INFORMATION

Corresponding Author

*E-mail: grojas@cim.sld.cu.

Notes

The authors declare no competing financial interest.

ACKNOWLEDGMENTS

We thank Y. Marichal for her excellent technical assistance. A. Carr and A. M. Hernandez kindly provided the ganglioside samples. Y. Fernandez-Marrero supervised mammalian cell expression experiments and provided chimeric 14F7. This work was supported by the Center of Molecular Immunology, by the Norwegian Cancer Foundation and by the University of Oslo.

REFERENCES

- (1) Hakomori, S. (2002) The glycosynapse. *Proc. Natl. Acad. Sci. U.S.A.* 9, 225–232.
- (2) Yamamoto, H., Tsuji, S., and Nagai, Y. (1990) Tetrasialoganglioside GQ1b reactive monoclonal antibodies: their characterization and application for quantification of GQ1b in some cell lines of neural and adrenal origin(s). *J. Neurochem.* 54, 513–517.
- (3) Kotani, M., Ozawa, H., Kawashima, I., Ando, S., and Tai, T. (1992) Generation of one set of monoclonal antibodies specific for a pathway ganglio-series gangliosides. *Biochim. Biophys. Acta* 1117, 97–103.
- (4) Mukerjee, S., Nasoff, M., and Glassy, M. (1998) Characterization of human IgG1 monoclonal antibody against gangliosides expressed on tumor cells. *Hybridoma* 17, 133–142.
- (5) Vazquez, A. M., Alfonso, M., Lanne, B., Karlsson, K. A., Carr, A., Barroso, O., Fernandez, L. E., Rengifo, E., Lanio, M. E., Alvarez, C., Zeuthen, J., and Perez, R. (1995) Generation of a murine monoclonal antibody specific for *N*-glycolylneuraminic acid-containing gangliosides that also recognizes sulfated glycolipids. *Hybridoma* 14, 551–556.
- (6) Carr, A., Mullet, A., Mazon, Z., Vazquez, A. M., Alfonso, M., Mesa, C., Rengifo, E., Perez, R., and Fernandez, L. E. (2000) A mouse IgG₁ monoclonal antibody specific for *N*-glycolyl GM3 ganglioside recognized breast and melanoma tumors. *Hybridoma* 19, 241–247.
- (7) Rojas, G., Talavera, A., Munoz, Y., Rengifo, E., Krengel, U., Angström, J., Gavilondo, J., and Moreno, E. (2004) Light chain shuffling results in successful phage display selection of functional prokaryotic-expressed antibody fragments to *N*-glycolyl GM3 ganglioside. *J. Immunol. Methods* 293, 71–83.
- (8) Tsuchida, T., Saxton, R. E., Morton, D. L., and Irie, R. F. (1987) Gangliosides of human melanoma. *J. Natl. Cancer Inst.* 78, 45–54.
- (9) Roque-Navarro, L., Chakrabandhu, K., de Leon, J., Rodriguez, S., Toledo, C., Carr, A., de Acosta, C. M., Hueber, A. O., and Perez, R. (2008) Anti-ganglioside antibody-induced tumor cell death by loss of membrane integrity. *Mol. Cancer Ther.* 7, 2033–2041.
- (10) Carr, A., Mesa, C., Arango, M. C., Vazquez, A. M., and Fernandez, L. E. (2002) *In vivo* and *in vitro* anti-tumor effect of 14F7 monoclonal antibody. *Hybridoma Hybridomics* 21, 463–468.
- (11) Hoon, D. S. B., Wang, Y., Sze, L., Kanda, H., Watanabe, T., Morrison, S. L., Morton, D. L., and Irie, R. F. (1993) Molecular cloning of a human monoclonal antibody reactive to ganglioside GM3 on human cancers. *Cancer Res.* 53, 5244–5250.
- (12) Irie, R. F., Ollila, D. W., O'Day, S., and Morton, D. L. (2003) Phase I pilot clinical trial of human IgM monoclonal antibody to ganglioside GM3 in patients with metastatic melanoma. *Cancer Immunol. Immunother.* 53, 110–117.
- (13) Azuma, Y., Ishikawa, Y., Kawai, S., Tsunenari, T., Tsunoda, H., Igawa, T., Iida, S., Nanami, M., Suzuki, M., Irie, R. F., Tsuchiya, M., and Yamada-Okabe, H. (2007) Recombinant human hexamer-dominant IgM monoclonal antibody to ganglioside GM3 for treatment of melanoma. *Clin. Cancer Res.* 13, 2745–2750.
- (14) Lee, K. J., Mao, S., Sun, C., Gao, C., Blixt, O., Arrues, S., Hom, L. G., Kaufmann, G. F., Hoffman, T. Z., Coyle, A. R., Paulson, J., Felding-Habermann, B., and Janda, K. D. (2002) Phage display selection of a human single-chain Fv antibody highly specific for melanoma and breast cancer cells using a chemoenzymatically synthesized GM3 carbohydrate antigen. *J. Am. Chem. Soc.* 124, 12439–12446.
- (15) Krengel, U., Olsson, L. L., Martinez, C., Talavera, A., Rojas, G., Mier, E., Angström, J., and Moreno, E. (2004) Structure and molecular interactions of a unique antitumor antibody specific for *N*-glycolyl GM3. *J. Biol. Chem.* 279, 5597–5603.
- (16) Chothia, C., and Lesk, A. M. (1987) Canonical structures for the hypervariable regions of immunoglobulins. *J. Mol. Biol.* 196, 901–917.
- (17) Rodriguez, M., Llanes, L., Perez, A., Perez, R., and Vazquez, A. M. (2003) Generation and characterization of an anti-idiotypic monoclonal antibody related to GM3 (NeuGc) ganglioside. *Hybridoma Hybridomics* 22, 307–314.
- (18) Wu, T. T., and Kabat, E. A. (1970) An analysis of the sequences of the variable regions of Bence Jones proteins and myeloma light chains and their implications for antibody complementarity. *J. Exp. Med.* 132, 211–250.
- (19) Gerstner, R. B., Carter, P., and Lowman, H. B. (2002) Sequence plasticity in the antigen-binding site of a therapeutic anti-HER2 antibody. *J. Mol. Biol.* 321, 851–862.
- (20) Vajdos, F. F., Adams, C. W., Breece, T. N., Presta, L. G., de Vos, A. M., and Sidhu, S. S. (2002) Comprehensive functional maps of the antigen-binding site of an anti-ErbB2 antibody obtained with shotgun scanning mutagenesis. *J. Mol. Biol.* 320, 415–428.
- (21) Iba, Y., Hayashi, N., Sawada, J., Titani, K., and Kurosawa, Y. (1998) Changes in the specificity of antibodies against steroid antigens by introduction of mutations into complementarity-determining regions of the VH domain. *Protein Eng.* 11, 361–370.
- (22) Korpimäki, T., Rosenberg, J., Virtanen, P., Lamminmäki, U., Tuomola, M., and Saviranta, P. (2003) Further improvement of broad specificity hapten recognition with protein engineering. *Protein Eng.* 16, 37–46.
- (23) Hirabayashi, Y., and Taniguchi, M. (1989) GM3 ganglioside as melanoma specific antigen and its biological function. *Hum. Cell* 2, 63–69.
- (24) Mütthling, J., Steuer, H., Peter-Katalinić, J., Marx, U., Bethke, U., Neumann, U., and Lehmann, J. (1994) Expression of gangliosides GM3 (NeuAc) and GM3 (NeuGc) in myelomas and hybridomas of mouse, rat and human origin. *J. Biochem.* 116, 64–73.
- (25) Carr, A., Mazon, Z., Alonso, D. F., Mesa, C., Valiente, O., Gomez, D. E., Perez, R., and Fernandez, L. E. (2001) A purified GM3 ganglioside conjugated vaccine induces specific, adjuvant-dependent and non-transient antitumor activity against B16 mouse melanoma *in vitro* and *in vivo*. *Melanoma Res.* 11, 219–227.
- (26) Rosok, M. J., Eghtedarzadeh-Kondri, M., Young, K., Bajorath, J., Glaser, S., and Yelton, D. (1998) Analysis of BR96 binding sites for antigen and anti-idiotypic by codon-based scanning mutagenesis. *J. Immunol.* 160, 2353–2359.

(27) Schoonbroodt, S., Steukers, M., Viswanathan, M., Frans, N., Timmermans, M., Wehnert, A., Nguyen, M., Ladner, R. C., and Hoet, R. M. (2008) Engineering antibody heavy chain CDR3 to create a phage display Fab library rich in antibodies that bind charged carbohydrates. *J. Immunol.* *181*, 6213–6221.

(28) Fernandez-Marrero, Y., Hernández, T., Roque-Navarro, L., Talavera, A., Moreno, E., Griñan, T., Vazquez, A. M., de Acosta, C. M., Perez, R., and Lopez-Requena, A. (2011) Switching on cytotoxicity by a single mutation at the heavy chain variable region of an anti-ganglioside antibody. *Mol. Immunol.* *48*, 1059–1067.

(29) Burley, S. K., and Petsko, G. A. (1986) Amino-aromatic interactions in proteins. *FEBS Lett.* *203*, 139–143.

(30) Biot, C., Buisine, E., and Rooman, M. (2003) Free-energy calculations of protein-ligand cation- π and amino- π interactions: from vacuum to protein like environments. *J. Am. Chem. Soc.* *125*, 13988–13994.

(31) Birtalan, S., Zhang, Y., Fellouse, F. A., Shao, L., Schaefer, G., and Sidhu, S. S. (2008) The intrinsic contributions of tyrosine, serine, glycine and arginine to the affinity and specificity of antibodies. *J. Mol. Biol.* *377*, 1518–1528.

(32) Marks, J. D., Hoogenboom, H. R., Bonnert, T. P., McCafferty, J., Griffiths, A. D., and Winter, G. (1991) By-passing immunization-human antibodies from V-gene libraries displayed on phage. *J. Mol. Biol.* *222*, 581–597.

(33) Coloma, M. J., Hasting, A., Wins, L. A., and Morrison, S. L. (1992) Novel vector for the expression of antibody molecules using variable regions generated by polymerase chain reaction. *J. Immunol. Methods* *52*, 89–104.

(34) Kunkel, T. A. (1985) Rapid and efficient site-specific mutagenesis without phenotypic selection. *Proc. Natl. Acad. Sci. U.S.A.* *82*, 488–492.

(35) Fellouse, F. A., and Sidhu, S. S. (2007). Making antibodies in bacteria, in *Making and Using Antibodies. A Practical Handbook* (Howard, G. C., and Kaser, M. R., Eds.) Chapter 8, pp 157–177, CRC Press, Boca Raton, FL.